Computer Communications 172 (2021) 35–44

Contents lists available at ScienceDirect

Computer Communications

journal homepage: www.elsevier.com/locate/comcom

Multi-windowed vertex-frequency analysis for signals on undirected graphs ☆

Xianwei Zheng [a,*], Cuiming Zou [b], Li Dong [c,1], Jiantao Zhou [d,e,2]

[a] School of Mathematics and Big Data, Foshan University, Foshan 528000, China
[b] College of Science, Huazhong Agricultural University, Wuhan 430070, China
[c] Department of Computer Science, Ningbo University, Zhejiang, China
[d] State Key Laboratory of Internet of Things for Smart City, University of Macau, Macau, China
[e] Department of Computer and Information Science, University of Macau, Macau, China

ARTICLE INFO

Keywords:
Graph signal
Windowed graph Fourier transform
Tight frames
Vertex frequency analysis

ABSTRACT

The recent emerging graph signal processing technologies have been widely applied to analyze signals defined on irregular domains, e.g., data collected from social networks, sensor networks, or transportation systems. Vertex frequency analysis, especially the windowed graph Fourier transform, is one of the most important tools for graph signal analysis and representations. Nevertheless, with a selected window function, it is rather challenging to construct tight frames via the windowed graph Fourier transform. To facilitate the construction of tight frames, in this paper, we consider multi-windowed graph Fourier transforms to develop novel vertex frequency analysis methods. Firstly, under the multi-windowed setting, tight graph Fourier frames are elaborately constructed to fulfill technical demands in different application scenarios. The canonical dual frames of the multi-windowed graph Fourier frames are investigated to establish the reconstruction formulas of graph signals. Additionally, we propose shift multi-windowed graph Fourier frames by directly using the shift operators, e.g., the adjacency matrix. The related tight frames, dual frames and their constructions are also discussed. Experimental results show that the proposed two types of frames can efficiently extract vertex-frequency features of synthetic graph signals. Furthermore, anomaly data can also be detected by these frames.

1. Introduction

As the explosion of information and communication in the modern society, data science is now facing a huge challenge to handle a variety of data analysis problems [1]. Among the real-world data, many types of signals are originally collected from distributed receivers or sensor networks, transportation or mobile networks [2,3], and internet of things [4,5], and thus naturally reside on an underlying irregular domain. Due to the complex irregular structures, classical signal processing techniques cannot be directly applied to analyze these structured data. Thus, it is of great importance to develop novel methodologies to handle signals with an underlying structure [6].

The recent emerging graph signal processing (GSP) theory redefines structured data as graph signals and provides novel perspectives for the processing of them [7]. Currently, the main focus of GSP is to build up systematic mechanisms for graph signals, similar to the classical signal processing theory [8]. The GSP theory contains a series of topics, like sampling theory [9,10], frequency analysis [11], topology inference [12,13], to name a few. For extracting and analyzing the vertex-frequency features of graph signals, the vertex-frequency analysis, which plays a role in GSP analogs to that of the time-frequency analysis in classical signal processing, has gradually become a hot topic in the GSP community. Specifically, the vertex-frequency analysis contains the graph Fourier transform, graph wavelet transform and filter-banks, windowed graph Fourier transform and the related frame theory [14].

The graph Fourier transform presents the spectral representations of graph signals and also sets the foundation for establishing the graph wavelet transform and windowed graph Fourier transform [15,16]. The graph wavelet transform can be applied to obtain multiscale and sparse representations of graph signals. The relevant variants of graph wavelet transform include multiscale or multiresolution transform

☆ This work was supported in part by the National Natural Science Foundation of China (Grant No. 61901116, Grant No. 61806027 and Grant No. 61901237); in part by the Guangdong Basic and Applied Basic Research Foundation, China (Grant No. 2019A1515010789); in part by the Macau Science and Technology Development Fund (Grant No. SKL-IOTSC-2018-2020, Grant No. 077/2018/A2, and Grant No. 0060/2019/A1); and in part by the Research Committee at the University of Macau (Grant No. MYRG2018-00029-FST and Grant No. MYRG2019-00023-FST).

* Corresponding author.
E-mail addresses: alexwzheng@fosu.edu.cn (X. Zheng), cmzou@mail.hzau.edu.cn (C. Zou), dongli@nbu.edu.cn (L. Dong), jtzhou@umac.mo (J. Zhou).
[1] Member, IEEE.
[2] Senior Member, IEEE.

https://doi.org/10.1016/j.comcom.2021.02.019
Received 26 December 2020; Received in revised form 31 January 2021; Accepted 21 February 2021
Available online 28 February 2021

[17,18], graph wavelet filter-banks [19–22], and adaptive multiscale transform [23,24]. Meanwhile, the windowed graph Fourier transform acts similar to the short time (windowed) Fourier transform in classical signal processing, and is applied to indicate local variations of graph signals in the vertex-frequency domain. In [16], the windowed graph Fourier transform was introduced under the framework of the graph Fourier transform and graph signal filtering. The key properties of windowed graph Fourier transform was then explored in [25], and the windowed graph Fourier frames were designed to extract vertex-frequency features of graph signals. The spectrum adapted windows were also designed to achieve better discriminative ability of the transform [26]. To accelerate the computation, fast algorithm for windowed graph Fourier transform was then constructed in [27]. Latter on, the theory was extended to vertex domain localization windows [28] and general Gabor-type frames [29]. The vertex-frequency representation given by the windowed graph Fourier frames could show the vertex-frequency feature of graph signals. But the reconstruction of the signal requires extra computation of a dual frame. By adopting tight frames, the dual frame could be ignored and extra computation of the dual frame would be saved. However, the problem of constructing tight windowed graph Fourier frames is still under exploring.

In this paper, based on our previous work [30], we extend the windowed graph Fourier transform to the multi-windowed case to facilitate the construction of tight frames. We present equivalent conditions for multi-windowed graph Fourier frames and tight frames. We also investigate the duals of multi-windowed graph Fourier frames to construct reconstruction formulas for any graph signals. To extend the scope of vertex-frequency analysis, we also define shift windowed graph Fourier frames. The related tight frames, duals and the key properties of them are also discussed. Experimental results show that the proposed multi-windowed and shift windowed graph Fourier frames are efficient in extracting vertex-frequency features of graph signals.

The rest of this paper is organized as follows: In Section 2, we briefly review the background of the paper. In Section 3, we introduce the definition of multi-windowed graph Fourier frames, and present some results on frames and tight frames. In Section 4, we give some results on the duals of multi-windowed graph Fourier frames. In Section 5, we define shift windowed graph Fourier frames and discuss the related duals and tight frames. In Section 6, we provide examples on constructing tight or near-tight multi-windowed and shift windowed graph Fourier frames. In Section 7, we present the experimental results. Section 8 concludes this work.

2. Background

In this section, we provide a brief overview of the notations and concepts from graph theory, graph signal processing, frame theory, time-frequency analysis and vertex-frequency graph signal analysis.

2.1. Notations and preliminaries

We denote an undirected weighted graph by $\mathcal{G} = (\mathcal{V}, \mathcal{E}, \mathbf{W})$, where $\mathcal{V}$ denotes the vertex set, $\mathcal{E}$ denotes edge set, and $\mathbf{W}$ denotes the adjacency matrix, respectively. If there exists an edge $e(i,j)$ connecting nodes i and j, $W_{i,j}$ is the weight value assign to the edge $e(i,j)$. We define the degree matrix $\mathbf{D}$ of $\mathcal{G}$ as a diagonal matrix whose ith diagonal element d_i is the degree of vertex i, i.e. the sum of the weights of all the edges incident to vertex i: $D_{ii} = \sum_j W_{ij}$. Then the graph Laplacian, also called the combinatorial graph Laplacian of $\mathcal{G}$ is defined as $\mathbf{L} = \mathbf{D} - \mathbf{W}$. Since $\mathcal{G}$ is undirected, $\mathbf{L}$ is a real symmetric matrix, and therefore has a complete set of orthonormal basis. Denote these eigenvectors by $\mathbf{u}_l$ for $l = 0, 1, \dots, N-1$, with associated eigenvalues λ_l, i.e. $\mathbf{L}\mathbf{u}_l = \lambda_l \mathbf{u}_l$. We denote the eigen-matrix by $\mathbf{U} = (\mathbf{u}_0, \mathbf{u}_1, \dots, \mathbf{u}_{N-1})$.

Then for any vector $\mathbf{f} \in \mathbb{R}^N$ defined on the vertices of $\mathcal{G}$, its graph Fourier transform $\widehat{\mathbf{f}}$ is defined by

$$\widehat{\mathbf{f}}(\lambda_l) = \langle \mathbf{f}, \mathbf{u}_l \rangle = \sum_{n=1}^{N} \mathbf{u}_l^*(n)\mathbf{f}(n).$$

The inverse transform can be derived by:

$$\mathbf{f}(n) = \sum_{l=0}^{N-1} \widehat{\mathbf{f}}(\lambda_l)\mathbf{u}_l(n).$$

The Parseval equation holds for the graph Fourier transform, that is, for any $\mathbf{f}, \mathbf{g} \in \mathbb{R}^N$, $\langle \mathbf{f}, \mathbf{g} \rangle = \langle \widehat{\mathbf{f}}, \widehat{\mathbf{g}} \rangle$.

2.2. Frames and operators [31]

Definition 2.1. A family of vectors $\{\mathbf{f}_k\}_{k=1}^M \subseteq \mathbb{R}^N$ $(M \geq N)$ is a finite frame for $\mathbb{R}^N$ if there exist constants $A, B > 0$, such that

$$A\|\mathbf{f}\|^2 \leqslant \sum_{k=1}^{M} \| \langle \mathbf{f}, \mathbf{f}_k \rangle|^2 \leqslant B\|\mathbf{f}\|^2$$

holds for every $\mathbf{f} \in \mathbb{R}^N$. The constants A and B are called frame bounds, and if $A = B$, $\{\mathbf{f}_k\}_{k=1}^M$ is called a tight frame.

For a frame $\{\mathbf{f}_k\}_{k=1}^M$, we define its associated synthesis operator $T : l^2(\mathbb{R}^N) \to \mathbb{R}^N$ by

$$T(\{c_k\}) = \sum_{k=1}^{M} c_k \mathbf{f}_k,$$

and the analysis operator $T^* : \mathbb{R}^N \to l^2(\mathbb{R}^N)$ by

$$T^*\mathbf{f} = \{\langle \mathbf{f}, \mathbf{f}_k \rangle\}.$$

Integrating T and T^* together, which are a pair of dual operators, we define the frame operator of $\{\mathbf{f}_k\}$ by $S = TT^*$, i.e.,

$$S\mathbf{f} = \sum_{k=1}^{M} \langle \mathbf{f}, \mathbf{f}_k \rangle \mathbf{f}_k, \mathbf{f} \in \mathbb{R}^N,$$

which is a bounded, positive, invertible and self-adjoint operator.

If there exists another sequence of vectors $\{\mathbf{g}_k\}_{k=1}^M$, such that

$$\mathbf{f} = \sum_{k=1}^{M} \langle \mathbf{f}, \mathbf{g}_k \rangle \mathbf{f}_k, \mathbf{f} \in \mathbb{R}^N,$$

we call $\{\mathbf{f}_k\}_{k=1}^M$ a dual frame of $\{\mathbf{f}_k\}_{k=1}^M$.

For any frame $\{\mathbf{f}_k\}_{k=1}^M$, it has an infinite number of dual frames. We could directly verify that $\{S^{-1}\mathbf{f}_k\}_{k=1}^M$ is a dual frame, which is often called the canonical dual frame of $\{\mathbf{f}_k\}_{k=1}^M$, where S^{-1} is the inverse of S.

Additionally, the synthesis operator of $\{\mathbf{f}_k\}_{k=1}^M$ can be written as a full rank $N \times M$ matrix $\mathbf{F}$, which has its columns as the frame elements, i.e., $\mathbf{F} = (\mathbf{f}_1, \mathbf{f}_2, \dots, \mathbf{f}_M)$. Then the analysis, frame operators and inverse frame operator of $\mathbf{F}$ can be represented as $\mathbf{F}^*$, $\mathbf{F}\mathbf{F}^*$ and $(\mathbf{F}\mathbf{F}^*)^{-1}$, respectively. Here $*$ denotes the matrix conjugate.

2.3. Short-time Fourier transform [32]

For any window function $g \in L^2(\mathbb{R})$ and $u \in \mathbb{R}$, the translation of g by u is defined by the operator T_u:

$$(T_u g)(t) := g(t-u). \tag{1}$$

For any $\xi \in \mathbb{R}$, the modulation of g by frequency ξ is defined by the operator M_ξ:

$$(M_\xi g)(t) := e^{2\pi i \xi t} g(t). \tag{2}$$

Given a finite sequence of window functions $g^1, \dots, g^L$, the family of discrete multi-windowed Fourier atoms is defined by:

$$\mathcal{G}^w = \{g^l_{m,n}(t) := (M_m T_n) g^l(t) = e^{2\pi i m t} g^l(t-n)\}, \tag{3}$$

where $l = 1, \dots, L$; $m \in \mathbb{Z}$; $n \in \mathbb{Z}$.

$\mathcal{G}^w$ is called a multi-windowed Fourier frame if there exist two positive constant $A, B > 0$, such that for any $f \in L^2(\mathbb{R})$,

$$A\|f\|^2 \leq \sum_{l=1}^{L} \sum_{m,n \in \mathbb{Z}} |\langle f, (M_m T_n) g^l \rangle|^2 \leq B\|f\|^2. \tag{4}$$

The constant A, B are called frame bounds. $\mathcal{G}_w$ is called a tight frame if $A = B$. Here $Sf(m,n,l) := \langle f, (M_m T_n) g^l \rangle = \int f(t)\overline{g^l(t-n)}e^{-2\pi mt}dt$ are the windowed Fourier transform coefficients. The coefficients $\{|Sf(m,n,l)|^2, l = 1,\dots,L\}_{m,n\in\mathbb{Z}}$ is generally called the "spectrogram" of signal f.

Any function $f \in L^2(\mathbb{R})$ can be reconstructed by using the windowed Fourier transform coefficients and a dual multi-windowed Fourier frame.

A multi-windowed Fourier frame $\tilde{\mathcal{G}}_L^w = \{\tilde{g}_{m,n}^l(t)\}$ generated by window functions $\tilde{g}^1,\dots,\tilde{g}^L$, is called a dual to $\mathcal{G}_L^w = \{g_{m,n}^l(t)\}$ if for any $f \in L^2(\mathbb{R})$,

$$f = \sum_{l=1}^{L}\sum_{m,n\in\mathbb{Z}} \langle f, (M_m T_n) g^l \rangle (M_m T_n)\tilde{g}^l. \tag{5}$$

2.4. Windowed graph Fourier transform for GSP [16]

For a graph signal $\mathbf{f} \in \mathbb{R}^n$ defined on a N-vertex graph $\mathcal{G} = (\mathcal{V}, \mathcal{E}, W)$, the generalized translation of $\mathbf{f}$ by i is defined by the operator T_i:

$$(T_i\mathbf{f})(n) := \sqrt{N}\sum_{p=0}^{N-1} \hat{\mathbf{f}}(p)\mathbf{u}_p^*(i)\mathbf{u}_p(n). \tag{6}$$

The generalized modulation of $\mathbf{f}$ by frequency k is defined by the operator M_k:

$$(M_k\mathbf{f})(n) := \sqrt{N}\mathbf{f}(n)\mathbf{u}_k(n). \tag{7}$$

The windowed graph Fourier atoms generated by a window function $\mathbf{g} \in \mathbb{R}^N$ on $\mathcal{G}$ are defined by

$$\mathbf{g}_{i,k}(n) := (M_k T_i \mathbf{g})(n) = N\mathbf{u}_k^*(n)\sum_{p=0}^{N-1} \hat{\mathbf{g}}(p)\mathbf{u}_p^*(i)\mathbf{u}_p(n), \tag{8}$$

with $i = 1,2,\dots,N$, $k = 0,1,\dots,N-1$. We denote the set of these windowed graph Fourier atoms by

$$\mathcal{G}^w = \{\mathbf{g}_{i,k}\}_{i=1,2,\dots,N;k=0,1,\dots,N-1}. \tag{9}$$

In [16] and [25], it was shown that the condition for a window $\mathbf{g} \in \mathbb{R}^N$ to generate a windowed graph Fourier frame is $\hat{\mathbf{g}}(0) \neq 0$.

Lemma 2.2. *For a window function $\mathbf{g} \in \mathbb{R}^N$ defined on $\mathcal{G}$, if $\hat{\mathbf{g}}(0) \neq 0$, then the windowed graph Fourier atoms defined in (9) is a frame with lower frame bound*

$$A := \min_{n\in\{1,2,\dots,N\}}\{N\|T_n\mathbf{g}\|_2^2\}, \tag{10}$$

and upper lower frame bound

$$B := \max_{n\in\{1,2,\dots,N\}}\{N\|T_n\mathbf{g}\|_2^2\}. \tag{11}$$

We then call the atom set a windowed graph Fourier frame (WGFF).

Constructing tight windowed graph Fourier frames is a valuable topic in GSP. By Lemma 2.2, technical design of window functions for tight frames would involve with complicated computations and analysis on the graph Fourier transform matrix. In the sequel, we utilize multi-window to construct tight frames and develop novel vertex-frequency analysis methods. As will be seen, multi-window could create more freedom than the single-window case and thus reduce the difficulty in the construction of tight frames.

3. Multi-windowed graph Fourier frames

Analog to (3) in the classical case, for a finite sequence of window functions $\mathbf{g}^1, \mathbf{g}^2, \dots, \mathbf{g}^L \in \mathbb{R}^N$, we can define the set of multi-windowed graph Fourier atoms by

$$\mathcal{G}_L^w = \{\mathbf{g}_{i,k}^l\}_{i=1,2,\dots,N;k=0,1,\dots,N-1;l=1,2,\dots,L}. \tag{12}$$

Theorem 3.1. *Let $\mathcal{G}_L^w$ be the set of multi-windowed graph Fourier atoms defined in (12). If $\sum_{l=1}^L |\hat{\mathbf{g}}^l(0)|^2 \neq 0$, then $\mathcal{G}_L^w$ is a frame with lower frame bound*

$$A := \min_{k\in\{1,2,\dots,N\}}\{N\sum_{l=1}^{L}\|T_n\mathbf{g}^l\|_2^2\}, \tag{13}$$

and upper lower frame bound

$$B := \max_{k\in\{1,2,\dots,N\}}\{N\sum_{l=1}^{L}\|T_n\mathbf{g}^l\|_2^2\}, \tag{14}$$

Proof. For any $\mathbf{f} \in \mathbb{R}^N$,

$$\begin{aligned}
&\sum_{l=1}^{L}\sum_{i=1}^{N}\sum_{k=0}^{N-1}|\langle \mathbf{f}, \mathbf{g}_{i,k}^l\rangle|^2 \\
&= \sum_{l=1}^{L}\sum_{i=1}^{N}\sum_{k=0}^{N-1}|\langle \mathbf{f}, M_k T_i \mathbf{g}^l\rangle|^2 \\
&= N\sum_{l=1}^{L}\sum_{i=1}^{N}\sum_{k=0}^{N-1}|\langle \mathbf{f}\circ(T_i\mathbf{g}^l)^*, u_k\rangle|^2 \\
&= N\sum_{l=1}^{L}\sum_{i=1}^{N}|\langle \mathbf{f}\circ(T_i\mathbf{g}^l), \mathbf{f}\circ(T_i\mathbf{g}^l)\rangle|^2 \\
&= N\sum_{l=1}^{L}\sum_{i=1}^{N}\sum_{n=1}^{N}|\mathbf{f}(n)|^2|(T_i\mathbf{g}^l)(n)|^2 \\
&= N\sum_{l=1}^{L}\sum_{i=1}^{N}\sum_{n=1}^{N}|\mathbf{f}(n)|^2|(T_n\mathbf{g}^l)(i)|^2 \qquad (15)\\
&= N\sum_{n=1}^{N}|\mathbf{f}(n)|^2\sum_{l=1}^{L}\|(T_n\mathbf{g}^l)\|_2^2,
\end{aligned}$$

where (15) follows from the symmetry of $\mathbf{L}$ and the definition of operator T_i in (6). In addition, if $\sum_{l=1}^L |\hat{\mathbf{g}}^l(0)|^2 \neq 0$, we have

$$\begin{aligned}
\sum_{l=1}^{L}\|T_n\mathbf{g}^l\|_2^2 &= N\sum_{p=0}^{N-1}\sum_{l=1}^{L}|\hat{\mathbf{g}}^l(p)|^2|\mathbf{u}_p(n)|^2 \\
&> \sum_{l=1}^{L}|\hat{\mathbf{g}}^l(0)|^2 > 0
\end{aligned} \tag{16}$$

By (16), taking the minimum and maximum of $\sum_{l=1}^L \|T_n\mathbf{g}^l\|_2^2$, we have the lower frame bound $A > 0$. Thus, $\mathcal{G}_L^w$ is a frame with lower and upper frame bounds defined in (13) and (14). □

We call the atom set defined in (12) a multi-windowed graph Fourier frame (MWGFF) if it forms a frame.

Let $c_n = N\sum_{l=1}^L \|T_n\mathbf{g}^l\|_2^2$ and $\mathbf{c} = (c_1,\dots,c_N)^T$, by the proof of Theorem 3.1, Eq. (15) shows that

$$\langle S\mathbf{f}, \mathbf{f}\rangle = \langle \mathbf{c}\circ\mathbf{f}, \mathbf{f}\rangle, \mathbf{f} \in \mathbb{R}^N. \tag{17}$$

Here $\circ$ denotes the entrywise product. That is, for vectors $\mathbf{c}$ and $\mathbf{f}$, the entrywise product $\mathbf{c}\circ\mathbf{f} = (c_1 f_1,\dots,c_N f_N)^T$.

Equivalently, we have

$$S\mathbf{f} = \mathbf{D}_c\mathbf{f}, \mathbf{f} \in \mathbb{R}^N, \tag{18}$$

where $\mathbf{D}_c = \mathrm{diag}(\mathbf{c})$ is a diagonal matrix, with its nth diagonal entry $D_{nn} = c_n = \sum_{l=1}^L \|T_n\mathbf{g}^l\|_2^2$.

Corollary 3.2. *$\mathcal{G}_L^w$ is a tight frame if and only if there exists a constant C, such that $N\sum_{l=1}^L \|T_n\mathbf{g}^l\|_2^2 = C$ for $n = 1,2,\dots,N$.*

Proof. From Eq. (18), the frame operator of $\mathcal{G}_L^w$ can be written as the diagonal matrix

$$S = \mathbf{D}_c = \mathrm{diag}(\mathbf{c}),$$

with $c_n = N\sum_{l=1}^L \|T_n\mathbf{g}^l\|_2^2$, $n = 1,\dots,N$. As the optimal lower and upper frame bounds of a frame are the smallest and largest eigenvalues of

the frame operator respectively, the frame bounds of $\mathcal{G}_L^w$ are given by the smallest and largest entries in $\mathbf{c}$. Therefore, $\mathcal{G}_L^w$ is a tight frame is equivalent to the condition that $\mathbf{c}$ is a constant vector, i.e. there exists a constant C, such that $c_n = C$ for $n = 1, 2, \dots, N$. □

Corollary 3.3. *Let $\mathcal{G}_L^w$ be the set of multi-windowed graph Fourier atoms defined in (12). If there exists a constant C, such that $\sum_{l=1}^{L} |\hat{\mathbf{g}}^l(\lambda_p)|^2 = C$, for $p = 0, 1, \dots, N-1$, then $\mathcal{G}_L^w$ is a tight frame with frame bounds $A = B = N^2C$.*

Proof. In the proof of Theorem 3.1, for any $f \in \mathbb{R}^N$, we have,

$$\sum_{l=1}^{L}\sum_{i=1}^{N}\sum_{k=0}^{N-1} |\langle \mathbf{f}, \mathbf{g}_{i,k}^l\rangle|^2 = N\sum_{n=1}^{N}|\mathbf{f}(n)|^2 \sum_{l=1}^{L}\|(T_n\mathbf{g}^l)\|_2^2$$
$$= N^2\sum_{n=1}^{N}|\mathbf{f}(n)|^2\sum_{p=0}^{N-1}\sum_{l=1}^{L}|\hat{\mathbf{g}}^l(\lambda_p)|^2|\mathbf{u}_p(n)|^2. \tag{19}$$

Since the eigen-matrix $\mathbf{U}$ of $\mathbf{L}$ is orthogonal, we have $\sum_{p=0}^{N-1}|\mathbf{u}_p(n)|^2 = 1$, for $n = 1, 2, \dots, N$. If $\sum_{l=1}^{L}|\hat{\mathbf{g}}^l(\lambda_p)|^2 = C$, for $p = 0, 1, \dots, N-1$, from Eq. (19), we have

$$\sum_{l=1}^{L}\sum_{i=1}^{N}\sum_{k=0}^{N-1}|\langle \mathbf{f}, \mathbf{g}_{i,k}^l\rangle|^2 = N^2C\|f\|_2^2. \tag{20}$$

Thus, $\mathcal{G}_L^w$ is a tight frame with frame bounds $A = B = N^2C$. □

Note that Corollary 3.3 presents a method for constructing multi-windowed graph Fourier tight frames. The details will be given in Section 6.

4. Dual of multi-windowed graph Fourier frames

In [25], the authors presented a reconstruction formula for single windowed graph Fourier frames. In this section, we provide a reconstruction formula by introducing the definition of dual of multi-windowed graph Fourier frames. Additionally, the canonical dual is also discussed.

Similar to the definition in (5), let $\tilde{\mathcal{G}}_L^w$ denotes the multi-windowed graph Fourier atom set generated by a finite sequence of window functions $\tilde{\mathbf{g}}^1, \tilde{\mathbf{g}}^2, \dots, \tilde{\mathbf{g}}^N$ in the sense of (12). $\tilde{\mathcal{G}}_L^w$ is called a dual to $\mathcal{G}_L^w$ if for any $\mathbf{f} \in \mathbb{R}^N$, there exists a constant C, such that

$$\mathbf{f} = C\sum_{l=1}^{L}\sum_{k=0}^{N-1}\sum_{i=1}^{N}\langle \mathbf{f}, \tilde{\mathbf{g}}_{i,k}^l\rangle\mathbf{g}_{i,k}^l = C\sum_{l=1}^{L}\sum_{k=0}^{N-1}\sum_{i=1}^{N}\langle f, \mathbf{g}_{i,k}^l\rangle\tilde{\mathbf{g}}_{i,k}^l. \tag{21}$$

Theorem 4.1. *Suppose that $\mathcal{G}_L^w$ is a multi-windowed graph Fourier frame as defined in (12). If there exists a finite sequence of window functions $\tilde{\mathbf{g}}^1, \tilde{\mathbf{g}}^2, \dots, \tilde{\mathbf{g}}^N$ and a constant $\mu > 0$, such that*

$$\sum_{l=1}^{L}\hat{\mathbf{g}}^l(\lambda_p)\hat{\tilde{\mathbf{g}}}^l(\lambda_p) = \mu,\ p = 0, 1, \dots, N-1, \tag{22}$$

then $\tilde{\mathcal{G}}_L^w$ is a dual of $\mathcal{G}_L^w$.

Proof. Suppose that $\sum_{l=1}^{L}\hat{\mathbf{g}}(\lambda_p)\hat{\tilde{\mathbf{g}}}(\lambda_p) = \mu$ for $p = 0, 1, \dots, N-1$. Then we have

$$\sum_{l=1}^{L}\sum_{i=1}^{N}\sum_{k=0}^{N-1}\langle \mathbf{f}, \mathbf{g}_{i,k}^l\rangle\tilde{\mathbf{g}}_{i,k}^l(n)$$
$$= \sum_{l=1}^{L}\sum_{i=1}^{N}\sum_{k=0}^{N-1}\Big(N\sum_{m=1}^{N}\mathbf{f}(m)\mathbf{u}_k^*(m)\sum_{p=0}^{N-1}\hat{\mathbf{g}}^l(\lambda_p)\mathbf{u}_p(i)\mathbf{u}_p^*(m)\Big)\cdot$$
$$\Big(N\mathbf{u}_k(n)\sum_{p'=0}^{N-1}\hat{\mathbf{g}}^l(\lambda_{p'})\mathbf{u}_{p'}^*(i)\mathbf{u}_{p'}(n)\Big)$$
$$= N^2\sum_{m=1}^{N}\mathbf{f}(m)\sum_{l=1}^{L}\sum_{p=0}^{N-1}\sum_{p'=0}^{N-1}\hat{\mathbf{g}}^l(\lambda_p)\hat{\tilde{\mathbf{g}}}^l(\lambda_{p'})\mathbf{u}_p^*(m)\mathbf{u}_{p'}(n)\cdot$$
$$\sum_{i=1}^{N}\mathbf{u}_p(i)\mathbf{u}_{p'}^*(i)\sum_{k=0}^{N-1}\mathbf{u}_k^*(m)\mathbf{u}_k(n)$$
$$= N^2\sum_{m=1}^{N}\mathbf{f}(m)\sum_{l=1}^{L}\sum_{p=0}^{N-1}\sum_{p'=0}^{N-1}\hat{\mathbf{g}}^l(\lambda_p)\hat{\tilde{\mathbf{g}}}^l(\lambda_{p'})\mathbf{u}_p^*(m)\mathbf{u}_{p'}(n)\delta_{pp'}\delta_{mn}$$
$$= N^2\mathbf{f}(n)\sum_{p=0}^{N-1}\sum_{l=1}^{L}\hat{\mathbf{g}}^l(\lambda_p)\hat{\tilde{\mathbf{g}}}^l(\lambda_p)|\mathbf{u}_p(n)|^2$$
$$= N^2\mu\mathbf{f}(n).$$

Here the orthogonality of $\mathbf{U}$ is applied in the last equation, i.e. $\sum_{p=0}^{N-1}|\mathbf{u}_p(n)|^2 = 1$. Thus, $\tilde{\mathcal{G}}_L^w$ is a dual of $\mathcal{G}_L^w$ with $C = N^2\mu$ in (21). □

We could also prove that the dual $\tilde{\mathcal{G}}_L^w$ of a multi-windowed graph Fourier frame $\mathcal{G}_L^w$ is also a frame.

Corollary 4.2. *Suppose that $\mathcal{G}_L^w$ is a multi-windowed graph Fourier frame as defined in (12). If there exists a finite sequence of window functions $\tilde{\mathbf{g}}^1, \tilde{\mathbf{g}}^2, \dots, \tilde{\mathbf{g}}^N$ and a constant $\mu > 0$, such that $\sum_{l=1}^{L}\hat{\mathbf{g}}^l(\lambda_p)\hat{\tilde{\mathbf{g}}}^l(\lambda_p) = \mu$ for $p = 0, 1, \dots, N-1$, then $\tilde{\mathcal{G}}_L^w$ is also a multi-windowed graph Fourier frame.*

Proof. If $\sum_{l=1}^{L}\hat{\mathbf{g}}^l(\lambda_p)\hat{\tilde{\mathbf{g}}}^l(\lambda_p) = \mu > 0$ for $p = 0, 1, \dots, N-1$, by the Cauchy–Schwartz inequality, we have

$$\mu^2 = |\sum_{l=1}^{L}\hat{\mathbf{g}}^l(\lambda_p)\hat{\tilde{\mathbf{g}}}^l(\lambda_p)|^2 \le \sum_{l=1}^{L}|\hat{\mathbf{g}}^l(\lambda_p)|^2\sum_{l=1}^{L}|\hat{\tilde{\mathbf{g}}}^l(\lambda_p)|^2, \tag{23}$$

for $p = 0, 1, \dots, N-1$. Then we have $\sum_{l=1}^{L}|\hat{\mathbf{g}}^l(\lambda_p)|^2 \neq 0$, and $\sum_{l=1}^{L}|\hat{\tilde{\mathbf{g}}}^l(\lambda_p)|^2 \neq 0$, for $p = 0, 1, \dots, N-1$. By Theorem 3.1, we have $\tilde{\mathcal{G}}_L^w$ is also a multi-windowed graph Fourier frame. □

Theorem 4.1 and Corollary 4.2 imply that there is a freedom on constructing dual multi-windowed graph Fourier frames. To be more specific, we could construct dual windows under Condition (22). For a multi-windowed graph Fourier frame $\mathcal{G}_L^w$ generated by $\mathbf{g}^1$, $\mathbf{g}^2$, ⋯, $\mathbf{g}^L \in \mathbb{R}^N$, the dual $\tilde{\mathcal{G}}_L^w$ can be constructed by selecting a constant μ then finding $\tilde{\mathbf{g}}^l \in \mathbb{R}^N$ by letting $\hat{\tilde{\mathbf{g}}}^l(\lambda_p) = \frac{\mu}{L\hat{\mathbf{g}}^l(\lambda_p)}$ for $p = 0, 1, \dots, N-1$. Condition (22) is then satisfied. But in case that $\hat{\mathbf{g}}^l(\lambda_k) = 0$ for some k and l, the dual cannot be constructed in this scheme. Consequently, it requires a technical design and calculation of the window functions. Additionally, in the multi-window case, the reconstruction formula require the dual frame generated by the dual windows, and thus would increase the computation for the reconstruction of signals.

Taking the diagonal property of the frame operator into accounts, we could easily obtain the canonical dual frame.

Corollary 4.3. *Suppose that $\mathcal{G}_L^w$ is a multi-windowed graph Fourier frame as defined in (12). Let $\mathbf{c} \in \mathbb{R}^N$ be a vector with $c_n = N\sum_{l=1}^{L}\|T_n\mathbf{g}^l\|_2^2$, and $\mathbf{d} \in \mathbb{R}^N$ be a vector with $d_n = \frac{1}{c_n}$, $n = 1, 2, \dots, N$. Then the canonical dual frame of $\mathcal{G}_L^w$ is given by*

$$\tilde{\mathcal{G}}_L^w := \{\tilde{\mathbf{g}}_{i,k}^l = \mathbf{d}\circ\mathbf{g}_{i,k}^l\}, \tag{24}$$

where $i = 1, 2, \dots, N; k = 0, 1, \dots, N-1; l = 1, 2, \dots, L$.

Proof. Suppose that S is the frame operator of $\mathcal{G}_L^w$. In the proof of Corollary 3.2, we have that

$$S = \mathbf{D}_c = \mathrm{diag}(\mathbf{c}).$$

According to Section 2.2, the canonical frame of $\mathcal{G}_L^w$ is then given by

$$S^{-1}\mathbf{g}_{i,k}^l = \mathbf{D}_c^{-1}\mathbf{g}_{i,k}^l = \mathbf{D}_d\mathbf{g}_{i,k}^l = \mathbf{d}\circ\mathbf{g}_{i,k}^l$$

where $i = 1, 2, \dots, N; k = 0, 1, \dots, N-1; l = 1, 2, \dots, L$. □

Remark that the dual frame $\tilde{\mathcal{G}}_L^w$ is unnecessary to be generated by a sequence of windows. Specifically, the graph translation operator does not commute with the entrywise product $\circ$, i.e.

$$T_i(\mathbf{c}\circ\mathbf{g}) \neq \mathbf{c}\circ T_i(\mathbf{g}), \mathbf{g} \in \mathbb{R}^N.$$

Even though the graph modulation operator commutes with the entry-wise product, i.e.

$$M_k(\mathbf{c}\circ\mathbf{g}) = \mathbf{c}\circ M_k(\mathbf{g}), \mathbf{g}\in\mathbb{R}^N,$$

we still have in general that,

$$M_k T_i(\mathbf{c}\circ\mathbf{g}) \neq \mathbf{c}\circ M_k T_i(\mathbf{g}), \mathbf{g}\in\mathbb{R}^N.$$

Finding the generator windows of a windowed graph Fourier frame could facilitate the investigation of the properties of the frame. However, without knowing the windows, the canonical dual frame can still be easily obtained from the original frame, and be applied to construct a reconstruction formula for graph signals.

5. Shift windowed graph Fourier frames

As the graph signal translation operator could increase the redundancy and complexity of the multi-windowed frame, an alternative is to take the graph shift operator as the translation operator. Given a graph $\mathcal{G} = (\mathcal{V}, \mathcal{E})$ with N vertices, the associated graph shift operator $\mathbf{S}$ is defined as an $N\times N$ matrix whose entry $S_{i,j}\neq 0$ only if $(i,j)\in\mathcal{E}$ [11]. The adjacency matrix is often utilized as a type of shift operator, acting like the translation operator in classical signal processing. By replacing the translation operator by the adjacency matrix in the multi-windowed graph Fourier atom set, we could then design a new type of multi-windowed frames.

Theorem 5.1. *Let $\{\mathbf{u}_i\}_{i=0}^{N-1}$ be the eigenvector of the Laplacian matrix of graph $\mathcal{G}$, with $\mathbf{A}$ be its adjacency matrix. Suppose that there are M window vectors $\mathbf{g}_l\in\mathbb{R}^N$, with $\mathbf{A}\mathbf{g}_l\neq 0$, $l=1,\dots,M$. Define*

$$\mathbf{g}_{i,l} := \mathbf{u}_i\circ(\mathbf{A}\mathbf{g}_l) \tag{25}$$

where $\circ$ denotes the entrywise product. Also define

$$\mathbf{c} = (c_1, c_2, \dots, c_N)^T, \text{with } c_k = \tilde{\mathbf{a}}_k\mathbf{G}\tilde{\mathbf{a}}_k^*, \tag{26}$$

where $\tilde{\mathbf{a}}_k$ is the kth row of matrix $\mathbf{A}$, and $\mathbf{G} = \sum_{i=1}^{L}\mathbf{g}_i\mathbf{g}_i^*$. The set of multi-window graph Fourier atoms

$$\mathcal{G}_L^s := \{\mathbf{g}_{i,l}\}_{i=0,2,\dots,N-1;l=1,2,\dots,M}. \tag{27}$$

forms a frame for signals defined on $\mathcal{G}$ if and only if $c_k>0$ for all of elements of $\mathbf{c}$. The optimal lower and upper frame bounds are

$$A = \min_{k\in\{1,2,\dots,N\}} c_k, \text{and}\quad B = \max_{k\in\{1,2,\dots,N\}} c_k, \tag{28}$$

respectively.

Proof. By the definition of the multi-window shift atoms, rewriting $\mathbf{g}_{i,l} := \mathbf{u}_i\circ(\mathbf{A}\mathbf{g}_l)$ in a matrix form, we have $\mathbf{g}_{i,l} = \mathbf{D}_i\mathbf{A}\mathbf{g}_l$, where $\mathbf{D}_i$ is a diagonal matrix with the kth diagonal entry equal to the kth element of $\mathbf{u}_i$. Let

$$\mathbf{T}_k = \left(\mathbf{D}_1\mathbf{A}\mathbf{g}_k, \mathbf{D}_2\mathbf{A}\mathbf{g}_k\cdots, \mathbf{D}_N\mathbf{A}\mathbf{g}_k\right), \tag{29}$$

the corresponding synthesis operator of $\mathcal{G}_L^s$ can be written as:

$$\mathbf{T} = \left(\mathbf{T}_1, \mathbf{T}_2\cdots, \mathbf{T}_M\right). \tag{30}$$

By Lemma, $\mathcal{G}_L^s$ forms a frame if and only if its frame operator is positive definite. In fact, the frame operator of $\mathcal{G}_L^s$ can be written as

$$\mathbf{T}\mathbf{T}^* = \sum_{l=1}^{M}\sum_{i=1}^{N}\mathbf{D}_i\mathbf{A}g_l g_l^*\mathbf{A}^*\mathbf{D}_i^*. \tag{31}$$

Note that for any diagonal matrix $\mathbf{D} = \text{diag}(\mathbf{u})$, and any matrix $\mathbf{M}$, we always have $\mathbf{D}\mathbf{M}\mathbf{D}^* = \mathbf{M}\circ(\mathbf{u}\mathbf{u}^*)$. Therefore, the frame operator $\mathbf{T}\mathbf{T}^*$ can be re-written as:

$$\begin{aligned}\mathbf{T}\mathbf{T}^* &= \sum_{l=1}^{M}\sum_{i=1}^{N}[\mathbf{A}g_l g_l^*\mathbf{A}^*]\circ(\mathbf{u}_i\mathbf{u}_i^*)\\ &= \sum_{l=1}^{M}\left[\left(\mathbf{A}g_l\right)\left(\mathbf{A}g_l\right)^*\right]\circ\left(\sum_{i=1}^{N}\mathbf{u}_i\mathbf{u}_i^*\right)\\ &= \sum_{l=1}^{M}\left[\left(\mathbf{A}g_l\right)\left(\mathbf{A}g_l\right)^*\right]\circ\mathbf{I}_N.\end{aligned} \tag{32}$$

Here $\mathbf{I}_N$ is the $N\times N$ identity matrix.

Let $\mathbf{G} = \sum_{i=1}^{L}\mathbf{g}_i\mathbf{g}_i^*$, we have

$$\sum_{l=1}^{M}\left(\mathbf{A}g_l\right)\left(\mathbf{A}g_l\right)^* = \mathbf{A}\mathbf{G}\mathbf{A}^*. \tag{33}$$

Eq. (32) indicates that $\mathbf{T}\mathbf{T}^*$ is a diagonal matrix with the kth diagonal entry given by the kth diagonal entry of $\mathbf{A}\mathbf{G}\mathbf{A}^*$. Let $\tilde{\mathbf{a}}_k$ be the kth row of matrix $\mathbf{A}$, by a simple matrix computation, the kth diagonal entry of $\mathbf{A}\mathbf{G}\mathbf{A}^*$ can be written as $c_k := \tilde{\mathbf{a}}_k\mathbf{G}\tilde{\mathbf{a}}_k^*$.

Recall that the optimal lower and upper frame bounds of a frame are the smallest and largest eigenvalues of the frame operator, respectively [31]. Therefore, $\mathcal{G}_L^s$ is a frame is equivalent to $c_k>0$ for all of elements of vector $\mathbf{c} = (c_1, c_2, \dots, c_N)^T$. The frame bounds of $\mathcal{G}_L^s$ can then be given by (28) which are the smallest and largest elements of $\mathbf{c}$ as defined in (26). □

Since the adjacency matrix in (27) can be replaced by any shift operator of graph signals. We call $\mathcal{G}_L^s$ a shift multi-windowed graph Fourier frame (SMWGFF) if the frame bounds in (28) can be obtained.

Similar to the multi-window graph Fourier frames, we can also derive the canonical dual frame in an entry-wise product manner.

Corollary 5.2. *Suppose that $\mathcal{G}_L^s$ is a shift multi-windowed graph Fourier frame as defined in (27). Let $\mathbf{c}\in\mathbb{R}^N$ be a vector with $c_k = \tilde{\mathbf{a}}_k\mathbf{G}\tilde{\mathbf{a}}_k^*$, and $\mathbf{d}\in\mathbb{R}^N$ be a vector with $d_n = \frac{1}{c_n}$, $n=1,2,\dots,N$. Then the canonical dual frame of $\mathcal{G}_L^s$ is given by*

$$\tilde{\mathcal{G}}_L^s = \{\tilde{\mathbf{g}}_{i,l} = \mathbf{d}\circ\mathbf{g}_{i,l}\}, \tag{34}$$

where $i=1,2,\dots,N; k=0,1,\dots,N-1; l=1,2,\dots,L$.

The proof of Corollary 5.2 is similar to Corollary 4.3, and is omitted. We could also derive an equivalent condition for the shift multi-windowed graph Fourier tight frames.

Corollary 5.3. *Let $\mathcal{G}_L^s$ be a shift multi-windowed graph Fourier frame, and $\tilde{\mathbf{a}}_k$ be the kth row of matrix $\mathbf{A}$. $\mathcal{G}_L^s$ is a tight frame if and only if*

$$\tilde{\mathbf{a}}_k\mathbf{G}\tilde{\mathbf{a}}_k^* = C, k=1,\dots,N, \tag{35}$$

where C is a constant number, and $\mathbf{G} = \sum_{i=1}^{L}\mathbf{g}_i\mathbf{g}_i^*$.

Proof. By Theorem 5.1, the frame bounds of $\mathcal{G}_L^s$ are given by the smallest and largest elements in $\mathbf{c}$, with $c_k = \tilde{\mathbf{a}}_k\mathbf{G}\tilde{\mathbf{a}}_k^*$.

Hence, $\mathcal{G}_L^s$ is a tight frame is then equivalent to $\tilde{\mathbf{a}}_k\mathbf{G}\tilde{\mathbf{a}}_k^* = C$ for $k=1,\dots,N$. □

According to Corollary 5.3, the construction of shift multi-windowed graph Fourier tight frames may be complicated. We discuss the construction of tight frames in the next section. In case that tight frames are not available, we construct near-tight frames.

6. Design of multi-windowed tight frames

In this section, we design two types of multi-windowed tight frames. We utilize the B-splines to construct the generator of tight multi-windowed graph Fourier frames (TMWGFF). Additionally, we construct tight shift multi-windowed graph Fourier frames (TSMWGFF) with N generators.

6.1. Construction of TMWGFF

Constructing TMWGFF is equivalent to find M generators $\{g_1, g_2, \dots, g_M\}$, such that, $\sum_{l=1}^{L} \|T_n \mathbf{g}^l\|_2^2 = C$ for $n = 1, 2, \dots, N$.

By Corollary 3.3, in the spectral domain, if $\sum_{l=1}^{L} |\hat{g}^l(\lambda_p)|^2 = C$, for $p = 0, 1, \dots, N-1$, $\mathcal{G}_L^w$ is tight frame in $\mathbb{R}^N$. Without lose of generality, we could let $C = 1$, the goal of the construction is to find a sequence of window functions, such that $\sum_{l=1}^{L} |\hat{g}^l(\lambda_p)|^2 = 1$, for $\lambda_p \in \sigma(\mathbf{L})$, where $\sigma(\mathbf{L})$ is the spectrum of the Laplacian matrix. That is, the modulus square of the generators form a partition of unity. As the generators should be localized, we could apply localized functions with the property of partition of unity to construct the generators. Among the functions with such a property, the cardinal B-splines are good candidates to be the generators.

The first order cardinal B-spline $\mathbf{N}_1$ is defined as the step function, i.e.

$$\mathbf{N}_1(x) = \begin{cases} 1 & x \in [0, 1], \\ 0 & \text{else.} \end{cases}$$

The kth order cardinal B-spline $\mathbf{N}_k$ is then defined in a recursive manner via convolution with $\mathbf{N}_1$, i.e.

$$\mathbf{N}_k(x) = \mathbf{N}_{k-1} * \mathbf{N}_1(x) = \int_0^1 \mathbf{N}_{k-1}(x-t)dt. \tag{36}$$

The integer-translates of the kth order cardinal B-spline form a partition of unity,

$$\sum_{p \in \mathbb{Z}} \mathbf{N}_k(x-p) = 1, \forall k \in \mathbb{N}^+. \tag{37}$$

In the following, we apply the kth order cardinal B-splines to construct the tight frame generators. Suppose that the spectrum of the Laplacian is $\sigma(\mathbf{L}) = [\lambda_A, \lambda_B]$, and the support set of $\mathbf{N}_k$ is $[c_k, d_k]$. Select a proper order k for the cardinal B-splines, such that $[c_k, d_k] \subset [\lambda_A, \lambda_B]$. As $\mathbf{N}_k$ is compact supported, we can find two integers k_1 and k_M, such that, when $k < k_1$ or $k > k_M$, $\mathbf{N}_k(x-k) = 0$, for $x \in [\lambda_A, \lambda_B]$. Correspondingly, the subsequence of integer translates of $\mathbf{N}_k$, $\{\mathbf{N}_k(x-k_1), \mathbf{N}_k(x-k_2), \dots, \mathbf{N}_k(x-k_M)\}$ form a partition of unity on $[\lambda_A, \lambda_B]$, where $k_1 < k_p \neq k_l < k_M$, for $1 < p, l < M$.

Let $|\hat{\mathbf{g}}_l(\lambda_p)|^2 = \mathbf{N}_k(\lambda_p - k_l)$ for $l = 1, 2, \dots, M$, we have

$$\sum_{l=1}^{M} |\hat{\mathbf{g}}_l(\lambda_p)|^2 = 1, \lambda_p \in [\lambda_A, \lambda_B]. \tag{38}$$

Thus, the window sequence $g_1, g_2, \dots, g_M$ generates a tight frame.

Remark that other types of functions that satisfy the property of partition of unity could be applied to construct TMWGFFs. The number of window functions is then depends on the support sets of the selected windows. The construction of tight frames by using other functions can be implemented similar to that of the cardinal B-splines.

6.2. Construction of TSMWGFF

As shown in Corollary 5.3, a SWGFF $\mathcal{G}_L^s$ with L windows, $\mathcal{G}_L^s$ is a tight frame is equivalent to $\tilde{\mathbf{a}}_k \mathbf{G} \tilde{\mathbf{a}}_k^* = C$ for $k = 1, \dots, N$. The condition can be rewritten as

$$\sum_{l=1}^{L} |\langle \tilde{\mathbf{a}}_k^T, \mathbf{g}_l \rangle|^2 = C. \tag{39}$$

The equations show that the modulus of projection of $\tilde{\mathbf{a}}_k$ in the subspace spanned by $\{\mathbf{g}_l\}_{l=1}^L$ are constant C.

Note that it is complicated and difficult to construct such a sequence of window vectors. But for a sequence of N windows, we can still construct tight or near-tight frames.

The goal is to construct $\mathbf{G} = \sum_{i=1}^{L} \mathbf{g}_i \mathbf{g}_i^*$ such that the matrix $\mathbf{AGA}^*$ has identical diagonal entries. Note that the diagonal entries of $\mathbf{AA}^*$ are the 2-norm of row vectors, i.e. $\|\mathbf{a}_k\|^2$ is the kth diagonal entry of $\mathbf{AA}^*$.

If $\|\mathbf{a}_k\|^2 = C$, for $k = 1, \dots, N$, we can select an orthonormal basis $\{\mathbf{u}_i\}_{i=1}^N$ in $\mathbb{R}^N$, and let $\mathbf{g}_i = \mathbf{u}_i$. We then have, $\|\mathbf{g}_l\| = 1$, $l = 1, 2, \dots, N$ and $\langle \mathbf{g}_k, \mathbf{g}_l \rangle = 0$, if $k \neq l$. As an orthonormal basis preserves 2-norm, we can still have

$$\sum_{l=1}^{N} |\langle \tilde{\mathbf{a}}_k^T, \mathbf{g}_l \rangle|^2 = \|\mathbf{a}_k\|^2 = C. \tag{40}$$

Thus, the window sequence $g_1, g_2, \dots, g_N$ generates a tight frame.

Otherwise, if $\|\mathbf{a}_k\|^2 \neq C$, for any $k \in \{1, \dots, N\}$, we could modified the orthonormal basis to construct tight or near-tight frames. We consider scaling the basis elements and let $\mathbf{g}_l = k_l \mathbf{u}_l$. The kth diagonal entry of matrix $\mathbf{AGA}^*$ is then become:

$$\sum_{l=1}^{N} |\langle \tilde{\mathbf{a}}_k^T, k_l \mathbf{u}_l \rangle|^2 = \sum_{l=1}^{N} k_l^2 |\langle \tilde{\mathbf{a}}_k^T, \mathbf{u}_l \rangle|^2. \tag{41}$$

Define a matrix $\mathbf{P}$, with $P_{k,l} = |\langle \tilde{\mathbf{a}}_k^T, \mathbf{u}_l \rangle|^2$, and a vector $\mathbf{x}$ with $x_l = k_l^2$, $k, l \in \{1, 2, \dots, N\}$. By Eq. (41), $g_1, g_2, \dots, g_N$ generate a tight frame is equivalent to

$$\mathbf{Px} = C\mathbf{1} \tag{42}$$

If Eq. (42) has a solution, $\{\mathbf{g}_l = k_l \mathbf{u}_l\}_{l=1}^N$ generates a tight frame. Otherwise, we can solve a minimization problem as follows:

$$\begin{aligned} \hat{\mathbf{x}} = \arg\min_{\mathbf{x}} \quad & \|\mathbf{Px} - C\mathbf{1}\|_2 \\ \text{subject to} \quad & \mathbf{x} \geq 0 \end{aligned} \tag{43}$$

The problem can be solved by using off-the-shelf convex optimization toolbox, e.g. the function lsqnonneg() in Matlab. The MWSGFF generated by $\{\mathbf{g}_l = k_l \mathbf{u}_l\}_{l=1}^N$ is then closest to be a tight frame in terms of the 2-norm distance.

Remark that in the construction of tight frames, MWGFF only related to the spectrum of the graph, while SMWGFF has a strong relationship with the shift operator, which often represents the graph topology. Both types of tight frames could be utilized in different scenarios when the spectral or topology property of the graph is considered.

7. Experiments

In this section, we present examples of tight frame window functions for MWGFF, and validate the performance of MWGFF and SMWGFF on extracting vertex frequency features of graph signals. The Matlab toolbox MatlabBGL [33] was applied.

7.1. Examples of tight frame window functions

We construct two sets of tight frame window functions based on the cardinal B-spline functions. As discussed in Section 6.1, we could utilize the cardinal B-spline functions to fulfill the condition that the spectral window functions forms a partition of unity on the spectrum of the graph.

Suppose that the normalized Laplacian matrix is applied, that is, the corresponding spectrum is contained in $[0, 2]$. We then taking the second order cardinal B-spline $\mathbf{N}_2$ to construct the tight frame window functions. By the recursive formula in (36), we have

$$\mathbf{N}_2(x) = \begin{cases} x & x \in [0, 1), \\ 1 - x & x \in [1, 2], \\ 0 & \text{else.} \end{cases}$$

Letting $|\hat{g}_1|^2 = \mathbf{N}_2(x-1)$, $|\hat{g}_2|^2 = \mathbf{N}_2(x)$, and $|\hat{g}_3|^2 = \mathbf{N}_2(x+1)$, according to Eq. (37), we have $\sum_{l=1}^{3} |\hat{g}_l(\lambda_p)|^2 = 1, \lambda_p \in [0, 2]$. That is, $\{g_1, g_2, g_3\}$ is a set of tight frame window functions. The spectral curves of the 3 window functions are presented in Fig. 1(a).

We could also improve the localization property of the tight frame window functions by utilizing the scaling of the cardinal B-spline functions. For example, letting $|\hat{g}_1|^2 = \mathbf{N}_2(2x-1)$, $|\hat{g}_2|^2 = \mathbf{N}_2(2x)$, $|\hat{g}_3|^2 = \mathbf{N}_2(2x+1)$, $|\hat{g}_4|^2 = \mathbf{N}_2(2x+2)$, and $|\hat{g}_5|^2 = \mathbf{N}_2(2x+3)$, we then have $\{g_1, g_2, g_3, g_4, g_5\}$ is a set of tight frame window functions. The

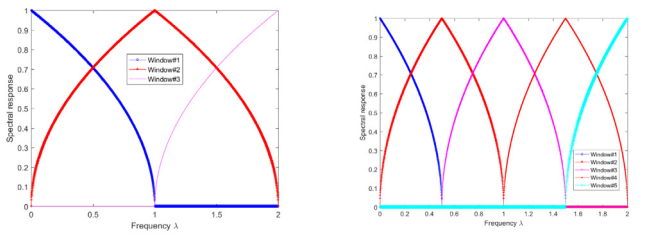

(a) (b)

Fig. 1. (a) Spectral curves of 3 tight frame B-spline window functions; (b) Spectral curves of 5 tight frame B-spline window functions.

spectral curves of the 5 window functions are given in Fig. 1(b), where each window function localized in a shorter interval on $[0, 2]$ than the window function in Fig. 1(a). Note that the number of windows is depends on the selected order of the cardinal B-spline functions or its scaling parameter. It may turn to an optimization on the optimal number of windows for specific application, which is beyond the scope of this work and could be discussed in our future work.

The construction of tight SMWGFF could be challenging. As discussed in Section 6.2, when the rows of the adjacency matrix have identical 2-norm values, we could construct orthonormal matrix as the window set. We design three types of orthonormal windows, which will be applied in the experiment later:

- the Laplacian eigenvectors, i.e. $\mathbf{g}_l = \mathbf{u}_{l-1}$, $l = 1, 2, \dots, N$, where $\mathbf{u}_l$ is the lth eigenvector of the Laplacian matrix.
- Householder vectors with localized generator, i.e. $\mathbf{g}_l = \mathbf{h}_l$, where $\mathbf{h}_l$ is the lth vector of the Householder matrix $\mathbf{H} = \mathbf{I}_N - 2\mathbf{v}\mathbf{v}^T$, and $\mathbf{v}$ is a vector localized on a small set of indices.
- translated vectors, i.e. $\mathbf{g}_i = T_i(\mathbf{g})$, $i = 0, 1, \dots, N-1$, $\mathbf{g}$ is a localized vector, and T_i is the translation operator of real-time vectors.

When the rows of the adjacency matrix have different 2-norm values, we could compute the vectors given by Model (43) for a set of N-windows, and then use them to generate a near-tight frame.

7.2. Vertex-frequency feature extraction

We then validate the performance of MWGFF and SMWGFF on extracting vertex frequency features of synthesis graph signals. The synthetic data are generated on path graph and sensor network by composing Laplacian eigenvectors.

In the first example, we consider an unweighted path graph of 100 vertices. We design a signal in Fig. 2(a) on the path graph by composing three Laplacian eigenvectors: u_8 restricted to the first 28 vertices, u_{18} restricted to the next 43 vertices, and u_{28} restricted to the remained vertices. The applied window function is the heat diffusion kernel, $\hat{g}(\lambda_l) = e^{-\tau\lambda_l}$ with $\tau = 80$, which is given in Fig. 2(b).

For comparison, we present the spectrograms generated by WGFF and SMWGFF, where each spectrogram consists of the squared magnitudes of the windowed graph Fourier frame coefficients. Fig. 2(c) shows that the vertex-frequency features of the signal can be precisely captured by the spectrograms generated by WGFF. Fig. 2(d) is the spectrogram generated by SMWGFF, with the window functions generated from the N-translations of the heat diffusion kernel, i.e. $\mathbf{g}_i = T_i(\mathbf{g})$, $i = 0, 1, \dots, N-1$ with $\tau = 2$,

$$\mathbf{g}(n) = \begin{cases} e^{-0.1\tau(n-1)} & 1 \le n \le 11, \\ 0 & n \ge 12. \end{cases} \tag{44}$$

The spectrogram of SMWGFF is also sensitive to the vertex-frequency features of the signal but less concentrated than the WGFF. The SMWGFF is more sensitive on the switching point of frequencies, as well as the dual of SMWGFF. As shown in Fig. 2(d) and (e), the two switching points are precisely marked by large frame coefficients. Fig. 2(f) is the spectrogram generated by the tightened SMWGFF. As can be observed, the tightened SMWGFF has better coefficient sparsity than the original SMWGFF and its dual.

In the second example, we validate the performance of MWGFF on a signal designed on sensor graph with 80 vertices in Fig. 3(a). The vertices of the graph is partitioned into 3 classes: red, blue and green. The applied MWGFF is generated by a set of 4 tight frame cardinal 2-order B-spline window functions, which are displayed in Fig. 3(b). Similar to the first example, the signal defined on this random graph is taken by restricting u_6 to the red vertices, u_{60} to the blue vertices, and u_{68} to the green vertices. Fig. 3(c) is the spectrogram generated by the first window that localized in the low frequency. Fig. 3(d), (e) and (f) are the spectrograms generated by the other 3 windows that localized in the central and high frequencies. The first spectrogram almost captures the vertex-frequency features of the signal around different frequencies and appropriate vertex sets. The last 3 spectrograms are less sensitive to the frequencies, but still giving proper localization on appropriate vertex sets.

In the third example, we validate the performance of SMWGFF by different generators given in Section 7(a) on a signal designed on sensor graph with 100 vertices in Fig. 4(a). The vertices of the graph is partitioned into 3 classes: red, blue and green. For comparison, we utilize two types of SMWGFF generators, the Laplacian eigen-matrix and the local Householder matrix. Similar to the first example, the signal defined on this random graph is taken by restricting u_8 to the red vertices, u_{18} to the blue vertices, and u_{28} to the green vertices. Fig. 4(b),(c) and (d) present the spectrograms generated by the SMWGFF with Householder matrix, its dual and the tightened SMWGFF, respectively. The local generator vector of the Householder matrix is given in Eq. (44). As can be seen, all the three spectrograms can capture the vertex-frequency feature around different frequencies and appropriate vertex sets, but slightly less localized than the WGFF. Additionally, the tightened SMWGFF in Fig. 4(d) has better sparsity than the other spectrograms. Fig. 4(e) presets the diagonal entries in the frame operators of the original SMWGFF and the tightened SMWGFF by the Laplacian eigen-matrix. It can be seen that the tightened SMWGFF is very close to be a tight frame as the diagonal entries are very close to be identical. In Fig. 4(f), (g), and (e), we present the spectrograms generated by the SMWGFF, its dual and the tightened SMWGFF, respectively, with respect to the Laplacian eigen-matrix. It shows that the spectrogram with respect to Laplacian eigen-matrix has better sparsity than that of the Householder matrix, but less localized in the frequency.

7.3. Anomaly detection

Finally, we apply the WGFF, MWGFF and SMWGFF to detect anomaly data in a graph signal. For that, we define a constant signal on the sensor graph with 100 vertices, by letting $f(n) = 0.1$, $n = 1, 2 \cdots, 100$. We then define the signal values of the neighbors of vertex v_{50} by letting $f(n) = 1$, $n \in \mathcal{N}(v_{50})$. The corresponding anomaly vertices are marked by blue bars in Fig. 5(b), (c) and (d). We compute the spectrogram of WGFF, MWGFF with 4 windows and SWGFF with the windows defined in (44). Taking maximum with respect to the vertices, the spectrogram coefficients then threshold by $\delta = 0.5 \cdot \max(\mathbf{S})$, where $\mathbf{S}$ denotes the spectrogram. The vertices with maximum coefficients larger than δ is then marked as red vertices. Fig. 5(a) is generated by WGFF spectrogram thresholding on the constant signal. As can be seen, about half of the vertices are detected as anomaly. In fact, the WGFF spectrogram coefficients of the constant signal are very close to their mean value. Using the δ thresholding could then misclassify about half of the vertices as anomaly. We present this result only for comparison and show that the spectrogram coefficients could then localized only on the anomalies for anomaly graph signals. In Fig. 5(b), the WGFF detected all the anomaly vertices but misclassified an extra vertex as anomaly. In Fig. 5(c), the SMWGFF spectrogram detected almost all except one anomalies, and also misclassified the same vertex as WGFF.

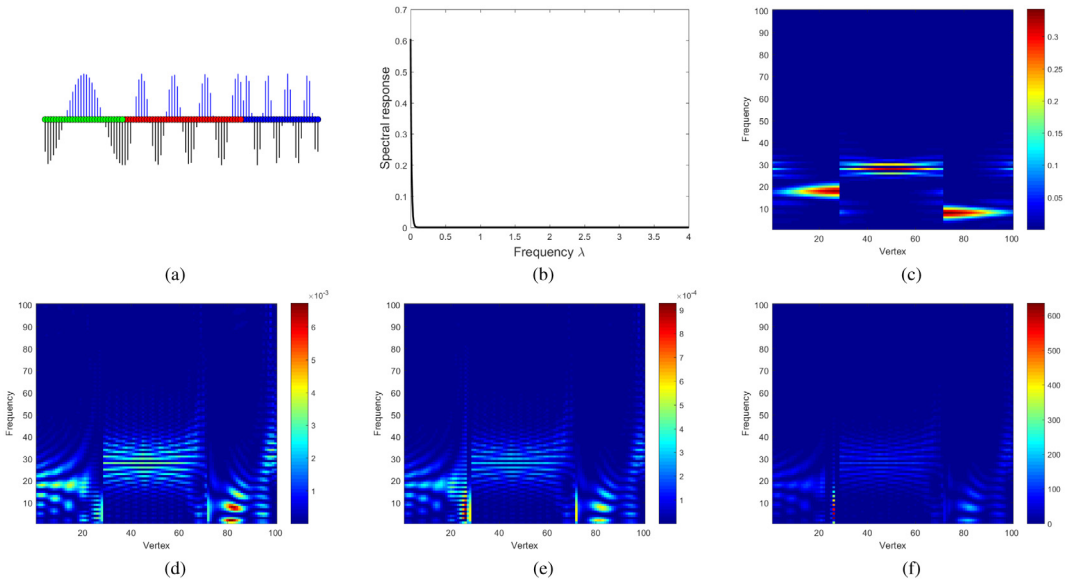

Fig. 2. (a) A signal on path graph by composing Laplacian eigenvectors; (b) The curves of the heat diffusion window function; (c) The spectrogram generated by WGFF; (d) The spectrogram generated by diffusion SMWGFF; (e) The spectrogram generated by dual diffusion SMWGFF; (f) The spectrogram generated by tightened diffusion SMWGFF.

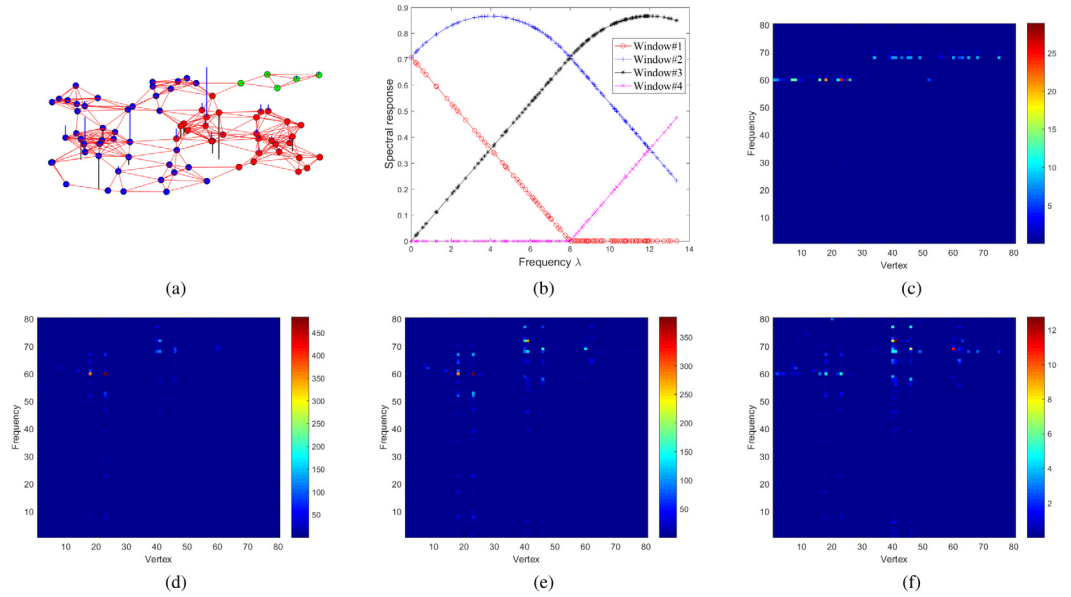

Fig. 3. (a) A signal on random graph by composing Laplacian eigenvectors; (b) The spectral curves of 4 tight frame window functions; (c) The spectrogram generated by window #1; (d) The spectrogram generated by window #2; (e) The spectrogram generated by window #3; (f) The spectrogram generated by window #4. (For interpretation of the references to color in this figure legend, the reader is referred to the web version of this article.)

In Fig. 5(d), we integrate the thresholding results on the spectrograms corresponding to the 4 windows of the MWGFF, by taking the union of anomalies given by the 4 spectrograms. It can be observed that the MWGFF integrated spectrogram detected all the anomaly vertices, and also detect the only vertex with degree 1 and its neighbor in the graph, which can also be considered as anomaly vertices. The MWGFF integrated spectrogram misclassifies 2 extra vertices as anomaly, which are actually neighbors of the anomalies. This example shows that MWGFF could be applied to find out the vertex-frequency features that both SMWGFF and WGFF unable to.

8. Conclusion

We extended the theory of windowed graph Fourier transform to the multi-windowed case. We presented conditions for constructing multi-windowed graph Fourier frames (MWGFF), tight frames and dual frames, respectively. We also propose shift multi-windowed graph Fourier frames (SMWGFF) and discuss the related dual and tight frames. Strategies for constructing tight or near tight MWGFF and SMWGFF are provided. We validate the performance of MWGFF and SMWGFF on extracting vertex-frequency features by experiments on synthesis graph signals. We also show that anomaly data on graph signals can be detected by MWGFF and SMWGFF.

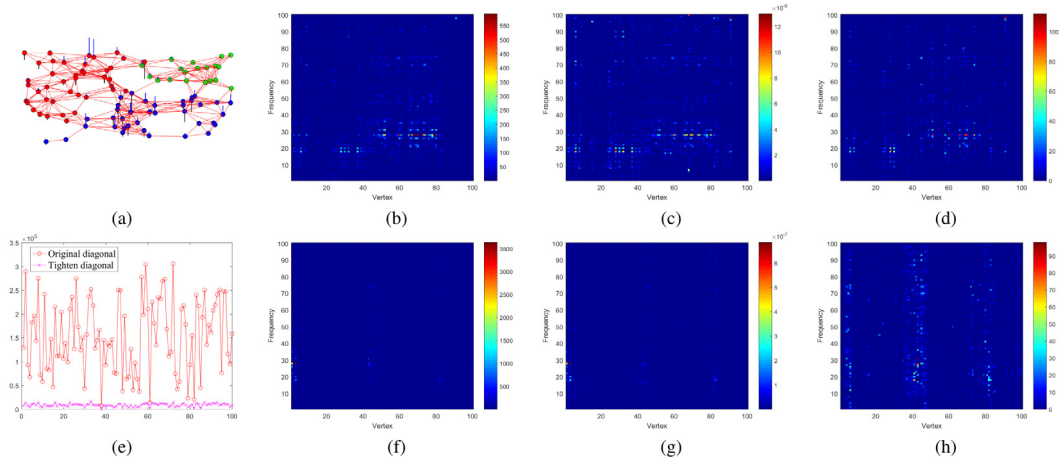

Fig. 4. (a) A graph signal by composing Laplacian eigenvectors; (b) The spectrogram generated by Householder SMWGFF; (c) The spectrogram generated by the dual of Householder SMWGFT; (d) The spectrogram generated by the tightened Householder SMWGFF; (e) The diagonal entries of the original and tightened frame operator; (f) The spectrogram generated by eigenmatrix SMWGFF; (g) The spectrogram generated by the dual of eigenmatrix SMWGFF; (h) The spectrogram generated by the tightened eigenmatrix SMWGFF. (For interpretation of the references to color in this figure legend, the reader is referred to the web version of this article.)

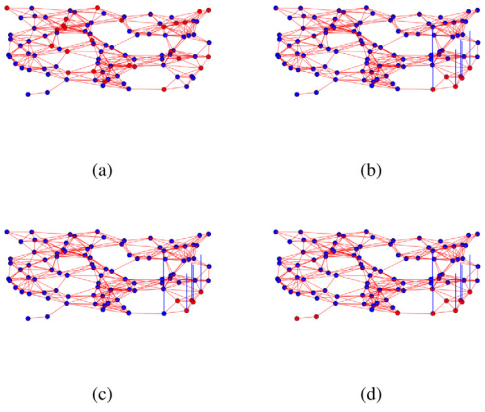

Fig. 5. (a) Anomaly vertices detected by the spectrogram on constant signal; (b) Anomaly vertices detected by the WGFF spectrogram on anomaly signal; (c) Anomaly vertices detected by the SMWGFF spectrogram on anomaly signal; (d) Anomaly vertices detected by the MWGFF integrated spectrogram on anomaly signal. (For interpretation of the references to color in this figure legend, the reader is referred to the web version of this article.)

CRediT authorship contribution statement

Xianwei Zheng: Methodology, Software, Writing- original draft. **Cuiming Zou:** Reviewing, Validation. **Li Dong:** Visualization, Writing - review & editing. **Jiantao Zhou:** Conceptualization, Resources.

Declaration of competing interest

The authors declare that they have no known competing financial interests or personal relationships that could have appeared to influence the work reported in this paper.

References

[1] A. Sandryhaila, J.M. Moura, Big data analysis with signal processing on graphs, IEEE Signal Process. Mag. 31 (5) (2014) 80–90.

[2] X. Han, G. Shen, X. Yang, X. Kong, Congestion recognition for hybrid urban road systems via digraph convolutional network, Transp. Res. C 121 (2020) 102877.

[3] W. Wang, F. Xia, H. Nie, et al., Vehicle trajectory clustering based on dynamic representation learning of internet of vehicles, IEEE Trans. Intell. Transp. Syst. (2020) 1–11, http://dx.doi.org/10.1109/TITS.2020.2995856.

[4] X. Kong, S. Tong, H. Gao, G. Shen, K. Wang, M. Collotta, I. You, S. Das, Mobile edge cooperation optimization for wearable Internet of Things: A network representation-based framework, IEEE Trans. Industr. Inform. (2020) http://dx.doi.org/10.1109/TII.2020.3016037.

[5] W. Wang, X. Zhao, Z. Gong, Z. Chen, N. Zhang, W. Wei, An attention-based deep learning framework for trip destination prediction of sharing bike, IEEE Trans. Intell. Transp. Syst. (2020) 1–11, http://dx.doi.org/10.1109/TITS.2020.3008935.

[6] A. Ortega, P. Frossard, J. Kovacevic, J.M.F. Moura, P. Vandergheynst, Graph signal processing: Overview, challenges, and applications, Proc. IEEE 106 (5) (2018) 808–828.

[7] D.I. Shuman, S.K. Narang, P. Frossard, A. Ortega, P. Vandergheynst, The emerging field of signal processing on graphs: Extending high-dimensional data analysis to networks and other irregular domains, IEEE Signal Process. Mag. 30 (3) (2013) 83–98.

[8] S. Mallat, A Wavelet Tour of Signal Processing: The Sparse Way, third ed., Academic Press, 2008.

[9] I.Z. Pesenson, M.Z. Pesenson, Sampling, filtering and sparse approximations on combinatorial graphs, J. Fourier Anal. Appl. 16 (6) (2010) 921–942.

[10] S. Chen, R. Varma, A. Sandryhaila, J. Kovacevic, Discrete signal processing on graphs: sampling theory, IEEE Trans. Signal Process. 63 (24) (2015) 6510–6523.

[11] A. Sandryhaila, J.M.F. Moura, Discrete signal processing on graphs: Frequency analysis, IEEE Trans. Signal Process. 62 (12) (2014) 3042–3054.

[12] S. Sardellitti, S. Barbarossa, P. Di Lorenzo, Graph topology inference based on sparsifying transform learning, IEEE Trans. Signal Process. 67 (7) (2019) 1712–1727.

[13] S. Segarra, A. Marques, G. Mateos, A. Ribeiro, Network topology inference from spectral templates, IEEE Trans. Signal Inf. Process. Netw. 3 (3) (2017) 467–483.

[14] L. Stanković, D. Mandic and, et al., Vertex-frequency graph signal processing: A comprehensive review, Digit. Signal Process. 107 (2020) 102802.

[15] D.K. Hammond, P. Vandergheynst, R. Gribonval, Wavelets on graphs via spectral graph theory, Appl. Comput. Harmon. Anal. 30 (2) (2011) 129–150.

[16] D.I. Shuman, B. Ricaud, P. Vandergheynst, A windowed graph Fourier transform, in: Proc. IEEE Stat. Signal Process. Workshop, Aug. 2012, pp. 133–136.

[17] D.I. Shuman, M.J. Faraji, P. Vandergheynst, A multiscale pyramid transform for graph signals, IEEE Trans. Signal Process. 64 (8) (2016) 2119–2134.

[18] J. Irion, S. Naoki, Applied and computational harmonic analysis on graphs and networks, in: Proc. SPIE 9597, Wavelets and Sparsity XVI, 95971F, 2015.

[19] S.K. Narang, A. Ortega, Perfect reconstruction two-channel wavelet filter banks for graph structured data, IEEE Trans. Signal Process. 60 (6) (2012) 2786–2799.

[20] S.K. Narang, A. Ortega, Compact support biorthogonal wavelet filterbanks for arbitrary undirected graphs, IEEE Trans. Signal Process. 61 (19) (2013) 4673–4685.

[21] Y. Tanaka, A. Sakiyama, M-channel oversampled graph filter banks, IEEE Trans. Signal Process. 62 (14) (2014) 3578–3590.

[22] D.B.H. Tay, J. Zhang, Techniques for constructing biorthogonal bipartite graph filter banks, IEEE Trans. Signal Process. 63 (21) (2015) 5772–5783.

[23] X.W. Zheng, Y.Y. Tang, J. Pan, J. Zhou, Adaptive multiscale decomposition of graph signals, IEEE Signal Process. Lett. 23 (10) (2016) 1389–1393.

[24] X.W. Zheng, Y.Y. Tang, J.T. Zhou, A framework of adaptive multiscale wavelet decomposition for signals on undirected graphs, IEEE Trans. Signal Process. 67 (7) (2019) 1696–1711.

[25] D.I. Shuman, B. Ricaud, P. Vandergheynst, Vertex-frequency analysis on graphs, Appl. Comput. Harmon. Anal. 40 (2) (2016) 260–291.

[26] D.I. Shuman, C. Wiesmeyr, N. Holighaus, et al., Spectrum-adapted tight graph wavelet and vertex-frequency frames, IEEE Trans. Signal Process. 63 (16) (2015) 4223–4235.
[27] I. Jestrović, J.L. Coyle, E. Sejdić, A fast algorithm for vertex-frequency representations of signals on graphs, Signal Process. 131 (2017) 483–491.
[28] L. Stanković, M. Dakovic, E. Sejdić, Vertex-frequency analysis: A way to localize graph spectral components [lecture notes], IEEE Signal Process. Mag. 34 (4) (2017) 176–182.
[29] M. Ghandehari, D. Guillot, K. Hollingsworth, Gabor-type frames for signal processing on graphs, 2020, [Online]. Available: http://arxiv.org/abs/2009.06058.
[30] X.W. Zheng, et al., Multi-windowed graph Fourier frames, in: Proc. IEEE International Conference on Machine Learning and Cybernetics, Vol. 2, 2016, pp. 1042–1048.
[31] P.G. Casazza, G. Kutyniok, Finite Frames: Theory and Applications, Springer, 2012.
[32] M. Zibulski, Y.Y. Zeevi, Analysis of multiwindow Gabor-type schemes by frame methods, Appl. Comput. Harmon. Anal. 4 (2) (1997) 188–221.
[33] D. Gleich, MatlabBGL, 2008, [Online]. Available: https://www.cs.purdue.edu/homes/dgleich/packages/matlab_bgl.